Neurobiology of Disease

Magnocellular Pathway Impairment in Schizophrenia: Evidence from Functional Magnetic Resonance Imaging

Antígona Martínez,[1,2] Steven A. Hillyard,[2] Elisa C. Dias,[1] Donald J. Hagler Jr,[2] Pamela D. Butler,[1] David N. Guilfoyle,[1] Maria Jalbrzikowski,[1] Gail Silipo,[1] and Daniel C. Javitt[1]

[1]Nathan S. Kline Institute for Psychiatric Research, Orangeburg, New York 10962, and [2]University of California, San Diego, La Jolla, California 92093

Sensory processing deficits in schizophrenia have been documented for several decades, but their underlying neurophysiological substrates are still poorly understood. In the visual system, the pattern of pathophysiology reported in several studies is suggestive of dysfunction within the magnocellular visual pathway beginning in early sensory cortex or even subcortically. The present study used functional magnetic resonance imaging to investigate further the neurophysiological bases of visual processing deficits in schizophrenia and in particular the potential role of magnocellular stream dysfunction. Sinusoidal gratings systematically varying in spatial frequency content were presented to subjects at low and high levels of contrast to differentially bias activity in magnocellular and parvocellular pathways based on well established differences in neuronal response profiles. Hemodynamic responses elicited by different spatial frequencies were mapped over the occipital lobe and then over the entire brain. Retinotopic mapping was used to localize the occipital activations with respect to the boundaries of visual areas V1 and V2, which were demarcated in each subject. Relative to control subjects, schizophrenia patients showed markedly reduced activations to low, but not high, spatial frequencies in multiple regions of the occipital, parietal, and temporal lobes. These findings support the hypothesis that schizophrenia is associated with impaired functioning of the magnocellular visual pathway and further suggest that these sensory processing deficits may contribute to higher-order cognitive deficits in working memory, executive functioning, and attention.

Key words: **schizophrenia; spatial frequency; fMRI; magnocellular; visual processing; retinotopy**

Introduction

Schizophrenia is a severe mental illness associated with complex and diverse impairments in cognitive, social, and affective behavior. Although most investigations into the neural basis of schizophrenia have focused on disturbances in higher-order brain regions such as prefrontal cortex (Cohen and Servan-Schreiber, 1992) or hippocampus (Achim et al., 2007), recent studies have also documented abnormalities in low-level sensory processes. In the visual system, for example, sensory processing deficits have been demonstrated using psychophysical measures of contrast sensitivity (Slaghuis, 2004; Butler et al., 2005) and motion detection (O'Donnell et al., 1996; Chen et al., 2004) as well as electrophysiological recordings of event-related potentials (ERPs) (Butler et al., 2007).

The early visual system consists of two basic subdivisions: a magnocellular division consisting of large, rapidly conducting neurons that project primarily to the dorsal visual stream and a parvocellular division consisting of smaller, more slowly conducting neurons projecting primarily to the ventral visual stream system. These two pathways can be differentiated on the basis of the distinctive functional properties of the constituent neurons (Kaplan, 1991; Merigan and Maunsell, 1993). Magnocellular neurons, for example, respond preferentially to low spatial frequency (SF) stimuli, whereas parvocellular neurons respond preferentially to high SFs. Magnocellular neurons are also differentially sensitive to motion and to low levels of luminance contrast. At low contrast, magnocellular neurons show nonlinear intensity functions, whereas parvocellular cells respond poorly but show linear responses at higher contrasts. Thus, at low contrast levels, visual information is conveyed to the cortex primarily via the magnocellular system, whereas both the magnocellular and parvocellular systems are engaged at higher contrasts with their relative contributions being dependent on stimulus parameters such as spatial frequency.

Visual processing impairments in schizophrenia have been attributed to preferential dysfunction within the magnocellular visual pathway. For example, schizophrenia patients have elevated contrast sensitivity thresholds, particularly to low-SF stimuli (Butler et al., 2001), as well as impaired sensitivity to vernier acuity (Kéri et al., 2005) and motion (O'Donnell et al., 1996; Chen et al., 1999a, 2004). Additionally, the amplitudes of sensory-evoked ERPs elicited by low, but not high, SFs are reduced in patients compared with control subjects (Butler et al., 2007). Findings from steady-state visual evoked potentials also suggest greater impairment to stimuli biased toward the magnocellular system using stimuli varying in either SF or saturating versus nonsaturating contrast increments (Butler et al., 2005).

Received March 2, 2008; revised June 9, 2008; accepted June 11, 2008.

This work was supported by National Institute of Mental Health Grant MH075849. We thank Raj Sangoi for technical assistance.

Correspondence should be addressed to Dr. Antígona Martínez, Nathan S. Kline Institute for Psychiatric Research, 140 Old Orangeburg Road, Orangeburg, NY 10962. E-mail: martinez@nki.rfmh.org.

DOI:10.1523/JNEUROSCI.1852-08.2008

 0270-6474/08/287492-09$15.00/0

Table 1. Sample characteristics of schizophrenia patients that participated in the study ($n = 13$)

Characteristic	Measurement (mean ± SEM)
Chlorpromazine daily equivalent (mg)	1326.7 ± 185.0
Antipsychotics	
Typical	2
Atypical	9
Combination	2
Illness duration (years)	18.5 ± 3.2
BPRS total score	37.2 ± 2.5
SANS total score	35.3 ± 4.5
GAF score	36.8 ± 3.0
IQ (Quick Test[a])	95.9 ± 2.9

BPRS, Brief Psychiatric Rating Scale; SANS, Scale for the Assessment of Negative Symptoms; GAF, Global Assessment of Functioning.

[a]Ammons and Ammons (1962).

The overall deficit pattern suggests that schizophrenia is associated with dysfunction at early cortical levels of the magnocellular pathway and perhaps even subcortically.

The present study investigated visual processing dysfunction in schizophrenia using stimuli designed to selectively bias activity of either the magnocellular or parvocellular visual pathways. Cortical activity elicited by horizontal gratings varying systematically in SF were analyzed using a phase-encoded approach to assess response selectivity within retinotopically defined visual areas. Relative to control subjects, schizophrenia patients differed dramatically in showing reduced responsiveness to low SFs. Furthermore, this group difference was most evident when the stimuli were delivered at low levels of contrast.

Materials and Methods

Subjects

Participants were 13 male patients (mean age, 36 ± 14 years) meeting DSM-IV criteria for schizophrenia ($n = 11$) or schizoaffective disorder ($n = 2$) and 11 healthy male volunteers (mean age 31 ± 11 years) (Table 1). Patients were recruited from inpatient and outpatient facilities associated with the Nathan Kline Institute for Psychiatric Research. Diagnoses were obtained using the Structured Clinical Interview for DSM-IV (SCID) (First et al., 1997) and all available clinical information. All patients were receiving antipsychotic medications at the time of testing. Healthy volunteers with a history of SCID-defined axis I psychiatric disorder were excluded. Patients and control volunteers were excluded if they had any neurological or ophthalmologic disorders that might affect performance, or if they met criteria for alcohol or substance dependence within the last 6 months or alcohol/substance abuse within the last month. All participants had at least 20/32 (0.63) corrected visual acuity or better on the Logarithmic Visual Acuity Chart (Precision Vision). Twelve of the patients and all control subjects were right handed.

Stimuli

All visual stimuli were presented to the subject during scanning via magnetic resonance-compatible liquid crystal display goggles (Resonance Technology).

Retinotopic mapping. The boundaries of retinotopically organized visual areas were defined using periodic stimuli similar to those described previously (Sereno et al., 1995). The stimuli consisted of high-contrast colored checks flickering at 8 Hz in counterphase as either a dilating/contracting ring (for eccentricity) or a rotating wedge (for polar angle). One full dilation/contraction or rotation cycle took 64 s, each scan consisted of eight cycles. At least two scans each for polarity and eccentricity mapping were acquired per subject.

Spatial frequency mapping. Stimuli were horizontal sinusoidal gratings that were continually counterphase reversing at 8 Hz. The gratings were formed on a 768 × 1024 pixel grid and occupied 9 × 12° of visual angle when viewed from within the magnet bore. Over the course of one 64 s cycle, the SF content of the gratings was monotonically increased from 0.2 to 4.9 cycles per degree (cpd) (Fig. 1). A single run consisted of eight cycles, with no delay between cycles. During one run, the gratings were presented at maximum contrast (close to 100%), and in a second run the contrast was reduced to 12%. A small fixation cross (10 × 10 pixels) was continuously visible at the center of each grating to aid in visual fixation. Every 4–10 s the fixation cross dimmed slightly, and subjects were required to make a button press response after detection of the change in luminance.

Image acquisition

T2*-weighted echoplanar images (EPIs) [repetition time (TR) = 2 s; echo time (TE) = 38 ms; flip angle = 90°; voxel size = 4 mm^3; matrix size = 64 × 64] were acquired on a 3T MRRS (formerly SMIS) 80 cm bore head-only magnetic resonance imaging (MRI) system housed at the Nathan Kline Institute Center for Advanced Brain Imaging. This system uses a 38 cm inner diameter (i.d.) gradient coil with gradient strength 40 mT/m, rise time of 280 μs, and a 30 cm i.d. transmission line radio frequency coil (Morris Instruments). During each run, 260 volumes were acquired on each of 32 contiguous slices in the axial plane. The first four volumes of each run (acquired before the onset of visual stimulation) were discarded before all analyses to allow for stabilization of the blood oxygen level-dependent (BOLD) signal. For anatomical localization of functional data and three-dimensional rendering of the cortical surface (see below), high-resolution (1 mm^3) images of the entire brain were acquired from each subject, using a standard magnetization-prepared rapid-acquisition gradient echo sequence (TR = 11.6 ms; TE = 4.9 ms; flip angle = 8°; effective inversion time = 1.1 s; matrix size = 256 × 256).

Data analysis

Anatomical image processing. A minimum of two high-resolution structural volumes were obtained from each subject in two or more scanning sessions. The images were manually registered using blink comparison (Sereno et al., 1995) and then averaged together to enhance the signal-to-noise ratio. A geometrical representation of each subject's cortical surface was rendered and unfolded. The posterior part of the unfolded brain surface, including the entire occipital lobe and parts of the parietal and temporal lobes, was then detached and flattened using cuts along the Sylvian fissure and along the fundus of the calcarine sulcus. All rendering and flattening procedures were implemented using FreeSurfer (http://surfer.nmr.mgh.harvard.edu/) and have been described in detail previously (Dale et al., 1999; Fischl et al., 1999).

Functional image processing. Processing of functional images was performed using a combination of the FreeSurfer and Analysis of Functional Neuroimages (AFNI) (Cox, 1996) software packages. Raw EPI images from individual subjects were motion corrected, linearly detrended, and slice time corrected before all analyses. Functional images were then coregistered with each individual's high-resolution anatomical images (obtained in the same scanning session) and projected to Talairach (Talairach and Tournoux, 1988) space before being spatially smoothed with a Gaussian kernel of 6 mm full-width at half-maximum.

Retinotopic maps. Retinotopic maps of eccentricity and polar angle were generated using FreeSurfer. The visual field sign of each visual area was calculated from these maps based on the direction of the fastest rate of change in polar angle and eccentricity with respect to cortical position (Sereno et al., 1994, 1995).

Spatial frequency maps. Cortical activity elicited by the spatial frequency gratings was assessed using the 3ddelay algorithm contained in the AFNI software suite. This algorithm uses the Hilbert transform and discrete Fourier transforms to estimate the temporal phase (i.e., response latency) and covariance of the functional MRI (fMRI) signal at each voxel with respect to a reference time series representing an ideal response with zero delay [for more details, see Saad et al. (2001, 2003)]. Because the SF content of the stimulus was varied systematically over time, the estimated response latency at any given voxel was directly related to the SF sensitivity of that cortical region. Thus, areas responding early during the stimulation cycle were sensitive to lower SFs, whereas areas responding at longer latencies were sensitive to higher SFs (Fig. 1).

Analyses of SF selectivity were primarily conducted within predefined regions of interest (ROIs). First, an ROI encompassing the entire occip-

ital lobe was anatomically defined on a template brain in Talairach coordinates. This ROI was used as a "mask" and applied to individual subject data (also in Talairach space) to exclude all brain regions falling outside the ROI. Second, separate ROIs of retinotopic areas V1 and V2 in each hemisphere were defined based on each subject's retinotopy.

Within each ROI, maps of the distribution of fMRI response latencies evoked by the periodic stimulus at 100 and 12% contrast levels were generated for each subject. These maps were used in voxelwise ANOVAs to test for significant group differences in SF selectivity. In all statistical tests, the significance levels and minimum voxel cluster size were calculated using a Monte Carlo simulation (AlphaSim written by B. D. Ward). Only voxels with F or t values corresponding to a p value of <0.01 (corrected for multiple comparisons) and belonging to a cluster of six or more contiguous voxels with significant responses survived the final threshold.

To simplify subsequent analyses, responses to SFs were grouped into four ranges corresponding to the lowest SFs (LSF: 0.2–1.4 cpd), medium-low SFs (MLSF: 1.5–2.5 cpd), medium-high SFs (MHSF: 2.5–3.4 cpd), and highest SFs (HSF: 3.5–4.9 cpd). For each individual subject, the number of voxels within each ROI with preferential responses in these four ranges was calculated. These voxel counts were subsequently entered into separate repeated-measures ANOVAs with a between-subject factor of group (patients, controls) and within-subject factors of contrast (100%, 12%) and SF range (LSF, MLSF, MHSF, HSF).

The magnitude of the BOLD signal in response to stimuli in each SF range was assessed by examining the covariance of each voxel's time series (relative to the reference time series) within the occipital ROI. The covariance of voxels with phase values indicating a preferential response to SFs in the LSF, MLSF, MHSF, and HSF ranges, at both levels of contrast, was calculated separately and averaged across subjects in each group. These values were subsequently used in separate t tests to test for significant between-group differences.

Contrast sensitivity functions

Contrast sensitivity (CS) functions were derived for all but two of the participants in the study (data were unavailable from one patient and one control) using previously described methods (for details, see Butler et al., 2005). Briefly, horizontal sine-wave gratings consisting of 0.5, 1, 2, 4, 7, or 21 cpd were delivered one at a time in random order to the left or right side of a computer screen. On each trial, the grating was presented for 32 ms, and subjects' task was to indicate which side of the screen the grating appeared in. An up–down transform response method (Wetherill and Levitt, 1965) was used to obtain contrast thresholds with a criterion of 70.7% correct responses for each SF. All data were analyzed as CS values, which is the reciprocal of the detection threshold. Group differences in CS were assessed in a repeated-

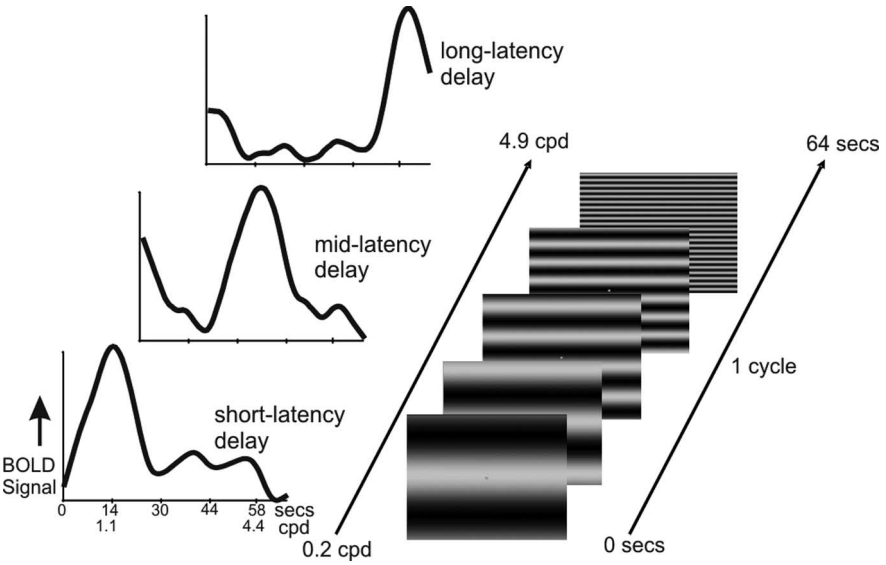

Figure 1. Stimuli and paradigm. Right, Continuously counterphase-reversing sinusoidal gratings were presented at fixation. In one cycle lasting 64 s, the gratings monotonically increased SF content from 0.2 to 4.9 cpd. Left, Analyses of SF selectivity were based on the BOLD signal response latency. Cortical regions with short response latencies were maximally sensitive to low SFs. Peak response latencies during the middle of the stimulation cycle correspond to preferred sensitivity to a mid-range SFs, and areas with long response latencies were maximally sensitive to high SFs.

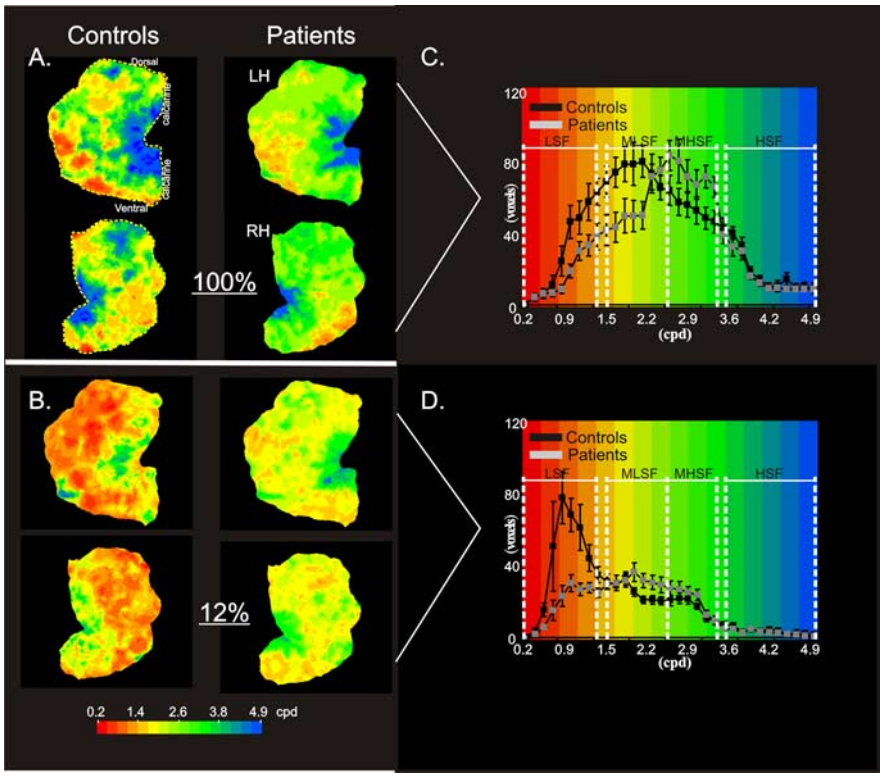

Figure 2. Differences between patients and controls in cortical areas activated by stimuli varying in SF. ***A***, Group-averaged response latency maps mapped onto a template of the occipital ROI (within dashed yellow lines) in Talairach coordinates. Color scale represents latency values corresponding to stimuli at different SFs (ranging from 0.2 to 4.9 cpd; see color scale below). Separate maps are shown for left (LH) and right (RH) hemisphere activations for control and patient groups in response to stimuli at 100% contrast. ***B***, Same as ***A*** for stimuli at low (12%) contrast. ***C***, Number of voxels within the occipital ROI (averaged across hemispheres and individuals in each group) with preferential responses at 100% contrast stimuli at different SFs. Corresponding ranges of SFs (LSF, MLSF, MHSF, and HSF) used in subsequent analyses are depicted in dashed white lines. ***D***, Same as ***C*** for the low (12%)-contrast stimuli.

Table 2. Mean number of voxels with peak responses in each of the four SF ranges tested (LSF, MLSF, MHSF, or HSF) and statistical significance of the comparison of controls (C) versus patients (P) for both levels of contrast

	LSF			MLSF			MHSF			HSF		
Contrast	C	P	*p*	C	P	*p*	C	P	*p*	C	P	*p*
100%	22	12	<0.003	56	44	<0.001	39	51	<0.005	13	11	NS
12%	34	14	<0.001	21	26	NS	12	14	NS	3	2	NS

measures ANOVA with between-subject factor of group (patients, controls) and a within-subject factor of SF (0.5, 1, 2, 4, 7, and 21 cpd).

The relationship between CS and fMRI measures of SF selectivity was evaluated across both groups of subjects using multiple regression analyses and simple linear correlations. In the regression analyses, the number of voxels in the occipital ROI with preferential responses to frequencies in the LSF (0.2–1.4 cpd) or HSF (3.5–4.9 cpd) range (collapsed across both levels of contrast) was used as a predictor for CS at the seven SFs tested. Linear correlations were then performed between the fMRI data and those CS values, which were significantly predicted by fMRI.

Results

Retinotopy

ROIs encompassing areas V1 and V2 were defined individually based on retinotopic mapping of the boundaries between these visual areas. The cortical extent of the V1 and V2 ROIs was ~15% lower in patients versus controls (V1/V2: 1649/1910 mm^2, controls; 1428/1684 mm^2, patients). This difference approached significance in V1 ($F_{(1,22)} = 3.50$; $p < 0.075$) but not in V2 ($F_{(1,22)} = 1.67$; $p < 0.210$).

Spatial frequency selectivity

Initial analyses were conducted within a large ROI encompassing the entire occipital lobe of both hemispheres (Fig. 2*A*, dashed line). Response latency maps for data collected at 100 and 12% contrast were averaged within each group of subjects. The resulting color maps shown in Figure 2, *A* and *B*, depict the topographic distribution of mean response latencies for each voxel in the ROI. These maps can alternatively be viewed as maps of SF sensitivity with each color in the scale representing a given SF delivered during the course of the periodic stimulation cycle.

At 100% contrast (Fig. 2*A*), both patients and controls showed preferential peak responses to high SFs predominantly around medial–occipital cortex and around the occipital pole (near the foveal representation). As the SF content of the stimulus was lowered, maximal responses were obtained in visual areas corresponding to progressively more peripheral retinal eccentricities and in more anterior and lateral regions of occipital cortex. At low (12%) contrast (Fig. 2*B*), responses in both subject groups were driven almost exclusively by low SFs and were restricted to peripheral retinal locations in early sensory regions as well as more anterior and lateral occipital regions.

The number of voxels with preferential responses to each SF was calculated individually and averaged across each group; graphs of these functions are shown in Figure 2, *C* and *D*, for high and low levels of contrast, respectively. These voxels were subsequently grouped into four bins (LSF, MLSF, MHSF, and HSF; see Materials and Methods). Within each SF bin, the average signal covariance was calculated for subjects in both groups and at both levels of contrast. At 100% contrast, the magnitude (covariance) of the BOLD signal elicited by HSF stimuli was significantly larger in patients versus controls ($t_{(22)} = 2.15$; $p < 0.041$). All other comparisons, at both 100% and 12% contrast, revealed no significant group differences ($p > 0.100$ for all).

The mean number of voxels with peak responses in each range of frequencies is shown in Table 2 for patients and controls. SF selectivity at high and low contrast was compared by testing the mean number of voxels with peak responses in each of the four SF ranges in a repeated-measures ANOVA. As expected, there was a significant overall contrast × SF interaction across groups ($F_{(3,66)} = 74.02$; $p < 0.001$). This interaction was attributable in part to a relatively larger number voxels sensitive to LSFs at low versus high contrast ($t_{(46)} = 3.45$; $p < 0.001$), consistent with the postulated preferential roles of the magnocellular and parvocellular pathways in mediation of low- versus high-SF responses, respectively.

Differences between patients and controls were evident as an overall significant main effect of group ($F_{(1,22)} = 8.80$; $p < 0.012$) as well as a group × SF interaction ($F_{(3,66)} = 27.30$; $p < 0.001$). This interaction was attributable in part to highly significant reductions in the number of voxels with activation in the LSF range in patients versus controls at both 100% ($t_{(22)} = 4.51$; $p < 0.001$) and 12% contrast ($t_{(22)} = 5.51$; $p < 0.001$), along with no significant group difference in the number of voxels with preferential sensitivity in the HSF range (100%: $t_{(22)} = 0.16$, $p > 0.900$; 12%:

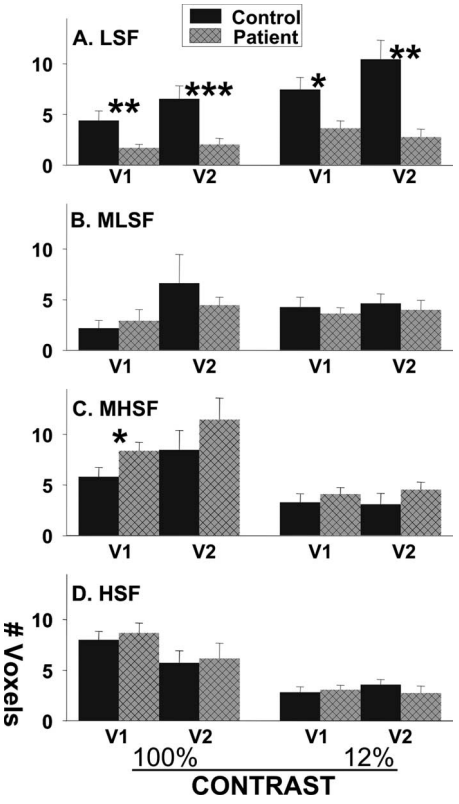

Figure 3. Mean number of voxels in retinotopically mapped areas V1 and V2 activated by LSF, MLSF, MHSF, and HSF stimuli at high contrast (left column) and low contrast (right column). Significant differences between controls (solid color) and patients (hatch pattern) are indicated by asterisks: *$p < 0.010$; **$p < 0.005$; ***$p < 0.001$. Error bars represent SEM.

$t_{(22)} = 0.12, p > 0.900$). Group differences in the MLSF and MHSF ranges were obtained at 100% but not 12% contrast. Specifically, whereas controls had a significantly larger number of MLSF-responsive voxels than patients ($t_{(22)} = 4.76$; $p < 0.001$), in the MHSF range, patients, rather than controls, activated more cortical area ($t_{(22)} = -3.11$; $p < 0.005$). Nonetheless, the most highly significant between-group difference was in the LSF range at 12% contrast, which maximally isolates the magnocellular visual pathway.

Subsequent preplanned ANOVAs were performed across the same SF ranges but restricted to ROIs encompassing visual areas V1 and V2. Across both visual areas and contrast levels, there was a significant group × SF interaction ($F_{(3,66)} = 9.67; p < 0.001$). Again, this interaction was principally attributable to a significantly larger proportion of voxels with preferential sensitivity to LSFs in the control group relative to patients (100% contrast: $t_{(22)} = 3.48, p < 0.002$; 12% contrast: $t_{(22)} = 3.94$, $p < 0.001$) (Fig. 3) with either no group differences or a reverse effect (for MHSF at 100% contrast) at higher SFs. These effects were comparable for areas V1 and V2 (group × SF × visual area interaction, $F_{(3,66)} = 0.82$, NS).

To further specify the cortical regions showing group differences in SF selectivity, analyses were performed across the entire range of SFs separately for each of the voxels within the occipital cortex ROI. Individual subject maps of voxel response latencies were entered into separate (100%, 12% contrast) one-way ANOVAs with a between-subject factor of group (patients, controls). At 100% contrast, significant group differences were obtained in the middle occipital gyrus (MOG), middle temporal gyrus (MTG), and lingual gyrus (LG) (Fig. 4, top; Table 3). In these regions, the group differences were attributable to patients having a significantly reduced number of voxels with preferential responses to low SFs compared with controls. Activations in an additional region corresponding to the precuneus (pCun) of the right hemisphere were also significantly different between groups because of a greater number of activated voxels to stimuli between ~3.0 and 3.7 cpd in the patient group. At low contrast, significant group differences were obtained in the superior occipital gyrus (SOG), MTG, LG, and pCun. As in the high-contrast condition, these group differences were largely attributable to fewer LSF-sensitive voxels in the patient group (Fig. 4, bottom; Table 3).

Finally, these same methods were used to test for differential SF sensitivity in patients versus controls in regions outside the occipital ROI (Fig. 5). At both levels of contrast, significant group differences ($p < 0.010$) were obtained in multiple regions of the temporal and parietal lobes (Fig. 5; Table 3, italicized regions), including the pCun, MTG, superior temporal gyrus, fusiform gyrus, and inferior parietal lobe. No areas of differential responsivity were observed in anterior brain regions. As in the occipital ROI areas, most of the group differences were attributable to larger LSF activations in the controls than in the patients.

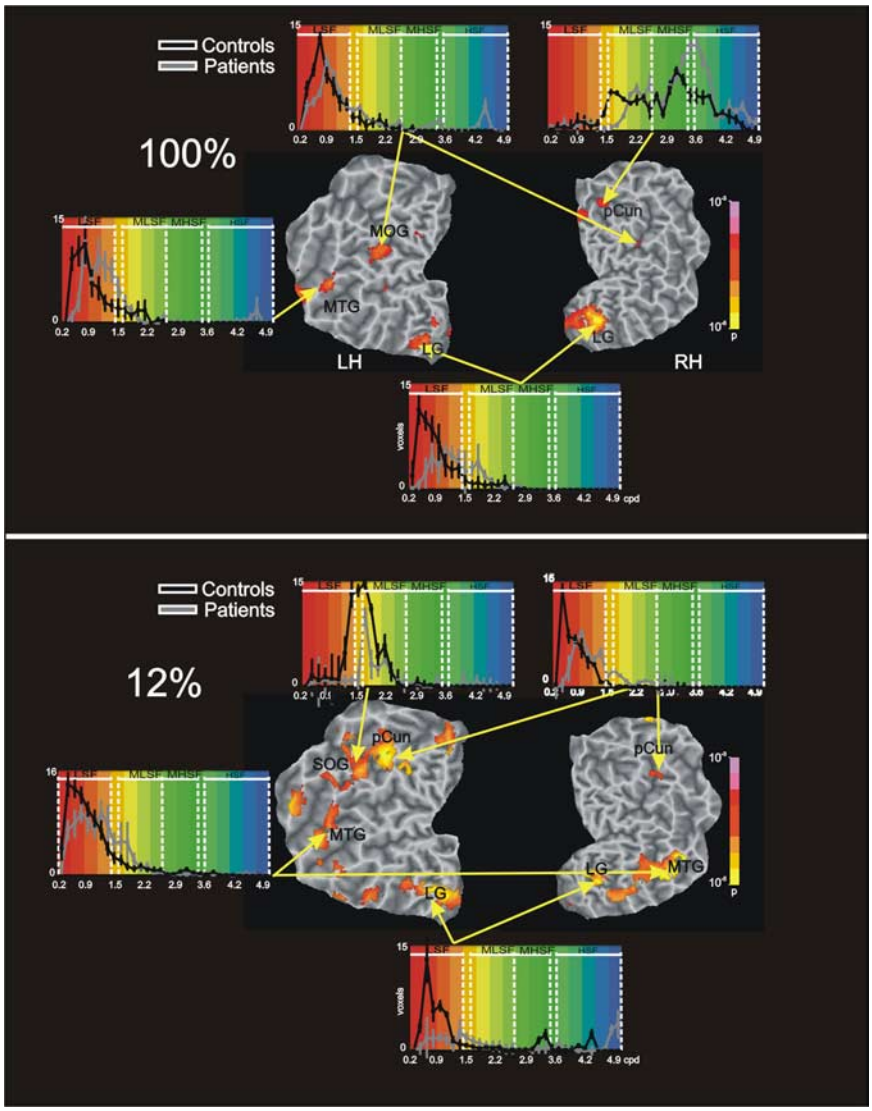

Figure 4. Cortical areas within the occipital ROI with significant group differences in SF selectivity. Maps of *p* values (see scales on right) are displayed on the left (LH) and right (RH) hemispheres of a template brain in Talairach coordinates for high (100%; top) and low (12%; bottom) contrast. The mean number of voxels showing peak responses at each SF within regions with a significant group difference is plotted for control subjects (black traces) and patients (gray traces).

Correspondence between fMRI and contrast sensitivity

Overall, patients showed reduced CS across all SFs (main effect of group: $F_{(1,22)} = 27.70$; $p < 0.001$). These deficits were greater at low (0.5, 1.0, and 2.0 cpd) versus high (4.0, 7.0, 10.0, and 21 cpd) SF, leading to a significant group × SF interaction ($F_{(6,132)} = 3.65$; $p < 0.002$).

When used as regressors in a multiple regression analysis, the LSF fMRI data significantly predicted CS at 0.5 cpd ($F_{(2,19)} = 10.42$; $p < 0.001$), 1.0 cpd ($F_{(2,19)} = 5.51$; $p < 0.012$), and 2.0 cpd ($F_{(2,19)} = 3.96$; $p < 0.036$) but not at higher SFs (all other $p > 0.100$). Linear correlations between the number of voxels with phase values corresponding to preferential responses to LSF stimuli and CS at 0.5, 1.0, and 2.0 cpd are shown in Figure 6. The HSF fMRI data were only significantly predictive of CS at 10.0 cpd ($F_{(2,19)} = 3.74$; $p < 0.043$; all other $p > 0.200$), which is higher

Table 3. Cortical areas inside and outside (italicized) the occipital ROI with significant differences in peak SF preference in schizophrenia patients versus control subjects

	x	*y*	*z*	Effect
100%				
Lft. mid. occ.	−27	−79	7	LSF: C > P
Rt. mid. occ.	27	−70	15	LSF: C > P
Rt. lingual (BA 19)	7	−62	1	LSF: C > P
Lft. lingual (BA 19)	−9	−60	0	LSF: C > P
Rt. precuneus	23	−50	21	MLSF: C > P; MHSF: P > C
Lft. mid. temp.	*−58*	*−46*	*−5*	LSF, MLSF: C > P
Lft. sup. temp.	*−54*	*−25*	*4*	LSF, MLSF: C > P
Lft. inf. par.	*−58*	*−27*	*21*	MLSF: C > P
12%				
Lft. cuneus/precuneus	−17	−78	28	LSF: C > P
Lft. sup. occ.	−27	−76	27	MLSF: C > P
Rt. lingual (BA 19)	14	−70	−7	LSF: C > P
Lft. lingual (BA 19)	−14	−66	3	LSF: C > P
Rt. precuneus	22	−63	39	LSF: C > P
Lft. mid. temp.	*−55*	*−56*	*−1*	LSF, MLSF: C > P
Rt. mid. temp.	*53*	*−56*	*−7*	LSF, MLSF: C > P
Lft. sup. temp.	*−52*	*−54*	*15*	LSF, MLSF: C > P
Rt. inf. temp.	*50*	*−54*	*−6*	LSF, MLSF: C > P
Rt. fusiform	*30*	*−51*	*−7*	LSF: C > P
Rt. precuneus	*9*	*−46*	*50*	LSF: C > P
Lft. inf. par.	*−30*	*−43*	*54*	LSF, MLSF: C > P
Rt. inf. par.	*49*	*37*	*40*	LSF, MLSF: C > P

For each area, the SF range (LSF, MLSF, MHSF, or HSF) accounting for the effect and direction of the effect is shown. Talairach coordinates correspond to site of maximum statistical significance. Lft., Left; mid., middle; Rt., right; sup., superior; inf., inferior; BA, Brodmann area; occ., occipital gyrus; lingual, lingual gyrus; temp, temporal gyrus; par., parietal lobe; C, control; P, patient.

than the highest SF included in the fMRI stimulus and did not significantly correlate with the fMRI data ($p > 0.500$).

Discussion

Visual processing deficits in schizophrenia have been well documented over the past 25 years, initially in the form of slowed visual integration and increased susceptibility to backward masking (Saccuzzo and Braff, 1981) and more recently in the form of reduced contrast sensitivity (Butler and Javitt, 2005) and reduced visual ERP amplitudes (Schechter et al., 2005; Butler et al., 2007). Despite behavioral and neurophysiological evidence of dysfunction within the visual system, some fMRI studies have shown normal (Braus et al., 2002; Barch et al., 2003) or even increased (Renshaw et al., 1994) activations the early (primary) visual cortex of patients compared with control subjects. A limitation of these studies, however, may be the nature of the stimuli used to produce visual activation, which were typically of high contrast and indeterminate SF content.

In the present study, we used stimuli that selectively biased activity of either the magnocellular or parvocellular systems. Our findings indicate that, relative to control volunteers, schizophrenia patients have deficits in response to magnocellular- but not parvocellular-biased stimuli. These deficits were evident in terms of the proportion of visual cortex with preferential responses to stimuli of varying SF content. Consistent with findings from other studies (Renshaw et al., 1994; Braus et al., 2002; Barch et al., 2003), the magnitude of the BOLD response in visual cortex did not generally differentiate patient from control subjects. However, the present study was not specifically designed for use of the BOLD signal as a primary measure of SF selectivity. To our knowledge, no studies thus far have examined BOLD signal change to magnocellular- versus parvocellular-biased stimuli; therefore, whether patients will show deficits to continuously presented low-contrast/low-SF stimuli, outside of a phase-encoded paradigm, remains an open question.

In general, the magnocellular system responds preferentially to low SFs, whereas the parvocellular system is more sensitive to higher SFs. Additionally, whereas high-contrast stimuli activate both magnocellular and parvocellular neurons, parvocellular cells respond poorly at contrast levels <16%. In the present study, stimuli were delivered across a broad range of spatial frequencies at either high or low contrast to selectively bias activity of the magnocellular and parvocellular pathways. The relative magnocellular/parvocellular biasing effect of these stimuli was reflected in control subjects by greater responsiveness to high SF (i.e., parvocellular) at 100% contrast versus 12% contrast and a significant increase in low-SF responses (i.e., magnocellular response) at 12 versus 100% contrast.

Compared with control subjects, schizophrenia patients showed diminished sensitivity to magnocellularly biased stimuli. In particular, the number of voxels with preferential responses to the lowest range of SFs was dramatically reduced in patients, especially at low contrast. Patients, on the other hand, had normal or even increased responses to middle-high- and high-SF stimuli. These fMRI measures of SF selectivity significantly predicted behavioral detection of simple visual stimuli. Specifically, diminished contrast sensitivity for magnocellularly biased stimuli was associated with a reduction in the extent of cortical volume with preferential responses to LSF stimuli, suggesting that early cortical dysfunction may play a critical role in visual behavioral deficits. For example, deficits in CS have been shown to contribute to dyslexia-like reading disturbances in schizophrenia patients (Revheim et al., 2006), further suggesting that deficits in early stages of visual processing may lead to secondary impairments in higher-order processing.

Reduced responsiveness to low-SF stimuli was observed in both striate and extrastriate visual areas, including MOG, MTG, and LG. These regions reportedly play a critical role in visual processes such as motion discrimination (Tootell et al., 1995), face processing (Puce et al., 1995; Narumoto et al., 2000), and reading (Pugh et al., 1996; Booth et al., 2001), all of which have been shown to be impaired in schizophrenia (Chen et al., 1999a, 2004; Manor et al., 1999; Herrmann et al., 2004; Revheim et al., 2006; Turetsky et al., 2007). Together, our findings thus suggest that the deficient responsiveness of the magnocellular pathways in schizophrenia patients may influence the operation of higher-order perceptual and cognitive systems.

The magnocellular pathway projects, through V1, preferentially to the dorsal visual processing stream. It has been proposed that the more rapid dorsal stream activation provides a critical "framing" input for ventral stream functions such as object recognition/perceptual closure and context-dependent processing (Schroeder et al., 1998; Vidyasagar, 1999; Doniger et al., 2002; Bar et al., 2006; Kveraga et al., 2007). Thus, dysfunction within the magnocellular pathway of schizophrenia patients may also underlie visual deficits that have been reported in object recognition and emotional processing (Doniger et al., 2001, 2002; Johnston et al., 2005; Turetsky et al., 2007).

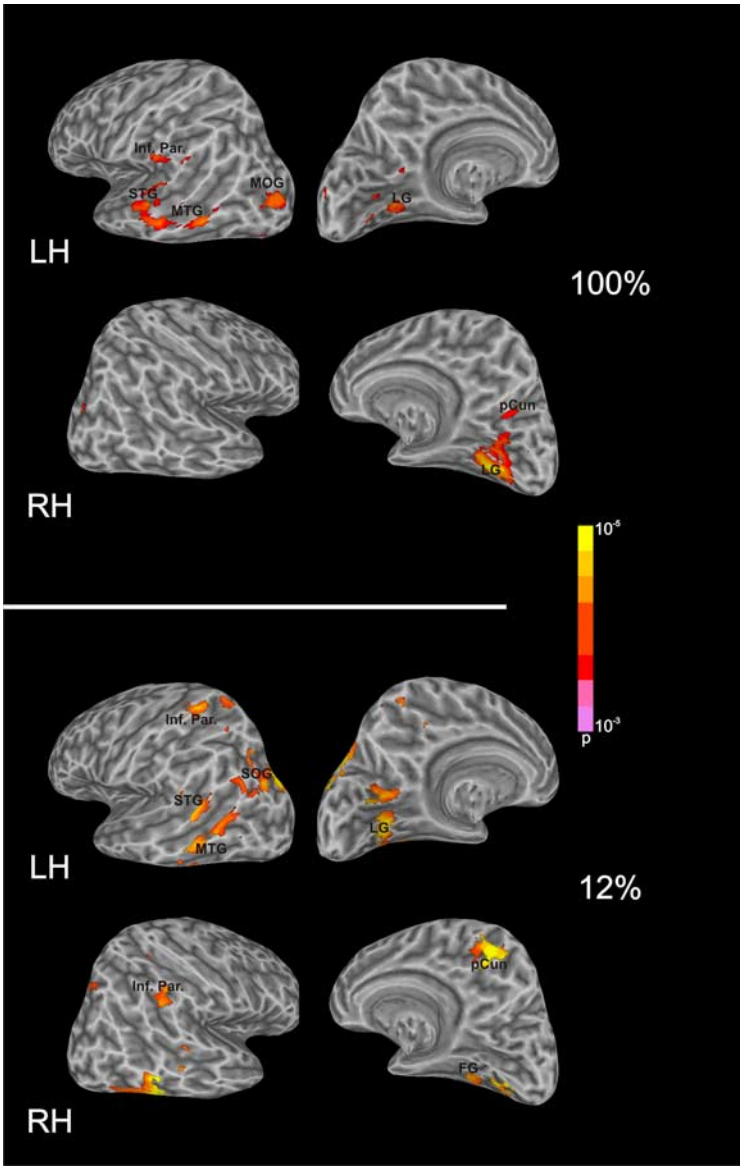

Figure 5. Whole-brain analysis of group differences in SF selectivity. Statistical significance maps resulting from the comparison of response latency maps for patients versus controls (*p* values; see scale on right) are displayed on the inflated left (LH) and right (RH) hemispheres of a template brain in Talairach coordinates for high- (100%; top) and low- (12%; bottom) contrast stimuli. For each hemisphere, the lateral (left column) and medial (right column) views are shown. FG, Fusiform gyrus; Inf. Par., inferior parietal lobe; STG, superior temporal gyrus.

The evidence presented here for a differential magnocellular deficit in schizophrenia is consistent with theories of generalized cortical/subcortical dysfunction in these patients. Although neuroimaging studies in schizophrenia have focused predominantly on higher-order cortical regions such as the dorsolateral prefrontal cortex or hippocampus, most current accounts of the origins of schizophrenia focus on genetic factors (e.g., neuregulin, dysbindin) or anatomical processes (e.g., dysmyelination, disconnectivity) that are present throughout the brain and, thus, do not predict the preferential involvement of specific cortical areas. In particular, magnocellular dysfunction might be expected if there were deficits in functioning of NMDA-type glutamate receptors in the visual pathways. NMDA receptors are known to play a prominent role in cortical gain control mechanisms within the magnocellular visual system (Kwon et al., 1992) with infusion of NMDA antagonists into LGN or primary visual cortex leading to reduced contrast-dependent cortical activation. The differential involvement of magnocellular versus parvocellular pathways in visual deficits in schizophrenia is thus consistent with an underlying dysfunction of NMDA receptors within subcortical and/or cortical visual pathways.

Although this study involved only chronic patients, visual processing deficits have been observed using behavioral measures in both medicated and unmedicated patients (Brody et al., 1980; Braff and Saccuzzo, 1982; Harvey et al., 1990; Butler et al., 1996, 2003) as well as in first-degree relatives of schizophrenia patients (Green et al., 1997; Chen et al., 1999b; Kéri and Janka, 2004) and in people with schizotypal personality disorder (Braff, 1981) who are not on medication. Similar findings have been reported using physiological measures of visual processing. For example, a recent fMRI study of (unmedicated) high-risk subjects who became symptomatic demonstrated abnormal activation patterns in the visual cortex of these subjects compared with that of high-risk subjects who remained asymptomatic (Whalley et al., 2006). Further, deficits in ERPs elicited by magnocellular-biased stimuli have been observed in family members of schizophrenia probands (Yeap et al., 2006), suggesting that early visual processing deficits may serve as an endophenotype for the disorder. Nonetheless, given the robustness of the visual processing abnormalities observed here in medicated patients, future studies in familial and symptomatic high-risk individuals are warranted.

In summary, the present study used an fMRI activation paradigm designed to isolate subcomponents of early visual processing in schizophrenia. Substantial deficits in magnocellular-mediated responses were observed, consistent with earlier behavioral and neurophysiological studies. Activation deficits were observed both in the retinotopic visual areas V1/V2 and in other regions of visual cortex normally responsive to low-SF stimuli. These findings are consistent with generalized theories of cortical/subcortical dysfunction in schizophrenia and, in particular, with predictions of the phencyclidine/NMDA model (Javitt, 2007).

References

Achim AM, Bertrand MC, Sutton H, Montoya A, Czechowska Y, Malla AK, Joober R, Pruessner JC, Lepage M (2007) Selective abnormal modulation of hippocampal activity during memory formation in first-episode psychosis. Arch Gen Psychiatry 64:999–1014.

Ammons R, Ammons C (1962) The Quick Test (QT): provisional manual. Psychol Rep 11:111–162.

Bar M, Kassam KS, Ghuman AS, Boshyan J, Schmid AM, Dale AM, Hämäläinen MS, Marinkovic K, Schacter DL, Rosen BR, Halgren E (2006) Top-down facilitation of visual recognition. Proc Natl Acad Sci U S A 103:449–454.

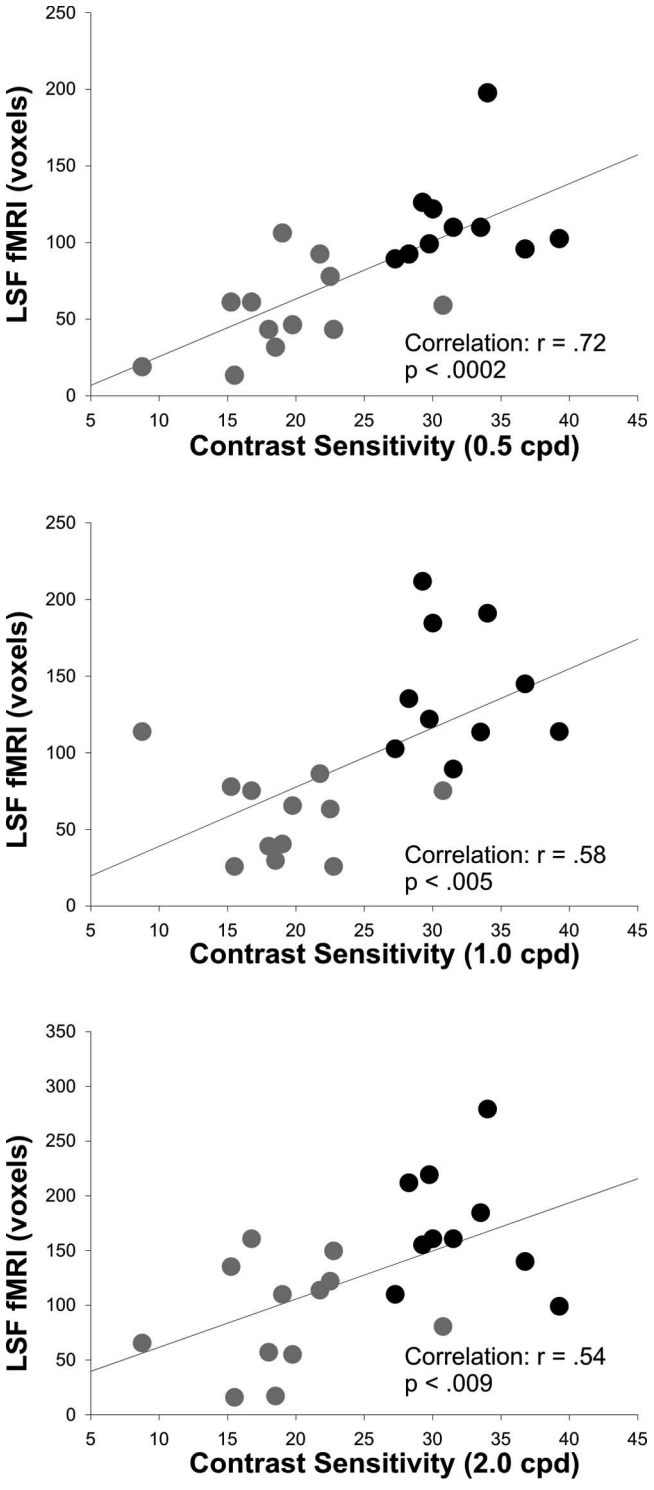

Figure 6. Scatterplots of correlation between CS and fMRI measures of SF selectivity. Linear correlations between the number of voxels with phase values corresponding to preferential responses to the LSF stimuli used in fMRI and individual CS values at 0.5 cpd (top), 1.0 cpd (middle), and 2.0 cpd (bottom) for patient (gray dots) and control (black dots) subjects.

Barch DM, Mathews JR, Buckner RL, Maccotta L, Csernansky JG, Snyder AZ (2003) Hemodynamic responses in visual, motor, and somatosensory cortices in schizophrenia. Neuroimage 20:1884–1893.

Booth JR, Burman DD, Van Santen FW, Harasaki Y, Gitelman DR, Parrish TB, Marsel Mesulam MM (2001) The development of specialized brain systems in reading and oral-language. Child Neuropsychol 7:119–141.

Braff DL (1981) Impaired speed of information processing in nonmedicated schizotypal patients. Schizophr Bull 7:499–508.

Braff DL, Saccuzzo DP (1982) Effect of antipsychotic medication on speed of information processing in schizophrenic patients. Am J Psychiatry 139:1127–1130.

Braus DF, Weber-Fahr W, Tost H, Ruf M, Henn FA (2002) Sensory information processing in neuroleptic-naive first-episode schizophrenic patients: a functional magnetic resonance imaging study. Arch Gen Psychiatry 59:696–701.

Brody D, Saccuzzo DP, Braff DL (1980) Information processing for masked and unmasked stimuli in schizophrenia and old age. J Abnorm Psychol 89:617–622.

Butler PD, Javitt DC (2005) Early-stage visual processing deficits in schizophrenia. Curr Opin Psychiatry 18:151–157.

Butler PD, Harkavy-Friedman JM, Amador XF, Gorman JM (1996) Backward masking in schizophrenia: relationship to medication status, neuropsychological functioning, and dopamine metabolism. Biol Psychiatry 40:295–298.

Butler PD, Schechter I, Zemon V, Schwartz SG, Greenstein VC, Gordon J, Schroeder CE, Javitt DC (2001) Dysfunction of early-stage visual processing in schizophrenia. Am J Psychiatry 158:1126–1133.

Butler PD, DeSanti LA, Maddox J, Harkavy-Friedman JM, Amador XF, Goetz RR, Javitt DC, Gorman JM (2003) Visual backward-masking deficits in schizophrenia: relationship to visual pathway function and symptomatology. Schizophr Res 59:199–209.

Butler PD, Zemon V, Schechter I, Saperstein AM, Hoptman MJ, Lim KO, Revheim N, Silipo G, Javitt DC (2005) Early-stage visual processing and cortical amplification deficits in schizophrenia. Arch Gen Psychiatry 62:495–504.

Butler PD, Martinez A, Foxe JJ, Kim D, Zemon V, Silipo G, Mahoney J, Shpaner M, Jalbrzikowski M, Javitt DC (2007) Subcortical visual dysfunction in schizophrenia drives secondary cortical impairments. Brain 130:417–430.

Chen Y, Levy DL, Sheremata S, Holzman PS (2004) Compromised late-stage motion processing in schizophrenia. Biol Psychiatry 55:834–841.

Chen Y, Palafox GP, Nakayama K, Levy DL, Matthysse S, Holzman PS (1999a) Motion perception in schizophrenia. Arch Gen Psychiatry 56:149–154.

Chen Y, Nakayama K, Levy DL, Matthysse S, Holzman PS (1999b) Psychophysical isolation of a motion-processing deficit in schizophrenics and their relatives and its association with impaired smooth pursuit. Proc Natl Acad Sci U S A 96:4724–4729.

Cohen JD, Servan-Schreiber D (1992) Context, cortex, and dopamine: a connectionist approach to behavior and biology in schizophrenia. Psychol Rev 99:45–77.

Cox RW (1996) AFNI—software for analysis and visualization of functional magnetic resonance neuroimages. Comput Biomed Res 29:162–173.

Dale AM, Fischl B, Sereno MI (1999) Cortical surface-based analysis I: segmentation and surface reconstruction. Neuroimage 9:179–194.

Doniger GM, Silipo G, Rabinowicz EF, Snodgrass JG, Javitt DC (2001) Impaired sensory processing as a basis for object-recognition deficits in schizophrenia. Am J Psychiatry 158:1818–1826.

Doniger GM, Foxe JJ, Murray MM, Higgins BA, Javitt DC (2002) Impaired visual object recognition and dorsal/ventral stream interaction in schizophrenia. Arch Gen Psychiatry 59:1011–1020.

First MB, Spitzer RL, Gibbon M, Williams JBW (1997) Structured clinical interview for DSM-IV axis I disorders—patient edition. New York: New York State Psychiatric Institute.

Fischl B, Sereno MI, Tootell RB, Dale AM (1999) High-resolution intersubject averaging and a coordinate system for the cortical surface. Hum Brain Mapp 8:272–284.

Green MF, Nuechterlein KH, Breitmeyer B (1997) Backward masking performance in unaffected siblings of schizophrenic patients. Evidence for a vulnerability indicator. Arch Gen Psychiatry 54:465–472.

Harvey PD, Keefe RS, Moskowitz J, Putnam KM, Mohs RC, Davis KL (1990) Attentional markers of vulnerability to schizophrenia: performance of medicated and unmedicated patients and normals. Psychiatry Res 33:179–188.

Herrmann MJ, Ellgring H, Fallgatter AJ (2004) Early-stage face processing dysfunction in patients with schizophrenia. Am J Psychiatry 161:915–917.

Javitt DC (2007) Glutamate and schizophrenia: phencyclidine, *N*-methyl-D-aspartate receptors, and dopamine-glutamate interactions. Int Rev Neurobiol 78:69–108.

Johnston PJ, Stojanov W, Devir H, Schall U (2005) Functional MRI of facial

emotion recognition deficits in schizophrenia and their electrophysiological correlates. Eur J Neurosci 22:1221–1232.

Kaplan E (1991) The receptive field structure of retinal ganglion cells in cat and monkey. In: Vision and visual dysfunction (Leventhal AG, ed), pp 10–40. Boston: CRC.

Kéri S, Janka Z (2004) Critical evaluation of cognitive dysfunctions as endophenotypes of schizophrenia. Acta Psychiatr Scand 110:83–91.

Kéri S, Kelemen O, Janka Z, Benedek G (2005) Visual-perceptual dysfunctions are possible endophenotypes of schizophrenia: evidence from the psychophysical investigation of magnocellular and parvocellular pathways. Neuropsychology 19:649–656.

Kveraga K, Boshyan J, Bar M (2007) Magnocellular projections as the trigger of top-down facilitation in recognition. J Neurosci 27:13232–13240.

Kwon YH, Nelson SB, Toth LJ, Sur M (1992) Effect of stimulus contrast and size on NMDA receptor activity in cat lateral geniculate nucleus. J Neurophysiol 68:182–196.

Manor BR, Gordon E, Williams LM, Rennie CJ, Bahramali H, Latimer CR, Barry RJ, Meares RA (1999) Eye movements reflect impaired face processing in patients with schizophrenia. Biol Psychiatry 46:963–969.

Merigan W, Maunsell J (1993) How parallel are the primate visual pathways? Annu Rev Neurosci 5:347–352.

Narumoto J, Yamada H, Iidaka T, Sadato N, Fukui K, Itoh H, Yonekura Y (2000) Brain regions involved in verbal or non-verbal aspects of facial emotion recognition. Neuroreport 11:2571–2576.

O'Donnell BF, Swearer JM, Smith LT, Nestor PG, Shenton ME, McCarley RW (1996) Selective deficits in visual perception and recognition in schizophrenia. Am J Psychiatry 153:687–692.

Puce A, Allison T, Gore JC, McCarthy G (1995) Face-sensitive regions in human extrastriate cortex studied by functional MRI. J Neurophysiol 74:1192–1199.

Pugh KR, Shaywitz BA, Shaywitz SE, Constable RT, Skudlarski P, Fulbright RK, Bronen RA, Shankweiler DP, Katz L, Fletcher JM, Gore JC (1996) Cerebral organization of component processes in reading. Brain 119:1221–1238.

Renshaw PF, Yurgelun-Todd DA, Cohen BM (1994) Greater hemodynamic response to photic stimulation in schizophrenic patients: an echo planar MRI study. Am J Psychiatry 151:1493–1495.

Revheim N, Butler PD, Schechter I, Jalbrzikowski M, Silipo G, Javitt DC (2006) Reading impairment and visual processing deficits in schizophrenia. Schizophr Res 87:238–245.

Saad ZS, Ropella KM, Cox RW, DeYoe EA (2001) Analysis and use of FMRI response delays. Hum Brain Mapp 13:74–93.

Saad ZS, DeYoe EA, Ropella KM (2003) Estimation of FMRI response delays. Neuroimage 18:494–504.

Saccuzzo DP, Braff DL (1981) Early information processing deficit in schizophrenia. New findings using schizophrenic subgroups and manic control subjects. Arch Gen Psychiatry 38:175–179.

Schechter I, Butler PD, Zemon VM, Revheim N, Saperstein AM, Jalbrzikowski M, Pasternak R, Silipo G, Javitt DC (2005) Impairments in generation of early-stage transient visual evoked potentials to magno- and parvocellular-selective stimuli in schizophrenia. Clin Neurophysiol 116:2204–2215.

Schroeder CE, Mehta AD, Givre SJ (1998) A spatiotemporal profile of visual system activation revealed by current source density analysis in the awake macaque. Cereb Cortex 8:575–592.

Sereno MI, McDonald CT, Allman JM (1994) Analysis of retinotopic maps in extrastriate cortex. Cereb Cortex 4:601–620.

Sereno MI, Dale AM, Reppas JB, Kwong KK, Belliveau JW, Brady TJ, Rosen BR, Tootell RB (1995) Borders of multiple visual areas in humans revealed by functional magnetic resonance imaging. Science 268:889–893.

Slaghuis WL (2004) Spatio-temporal luminance contrast sensitivity and visual backward masking in schizophrenia. Exp Brain Res 156:196–211.

Talairach J, Tournoux P (1988) Co-planar stereotaxic atlas of the human brain: 3-dimensional proportional system: an approach to cerebral imaging. New York: Thieme.

Tootell RB, Reppas JB, Kwong KK, Malach R, Born RT, Brady TJ, Rosen BR, Belliveau JW (1995) Functional analysis of human MT and related visual cortical areas using magnetic resonance imaging. J Neurosci 15:3215–3230.

Turetsky BI, Kohler CG, Indersmitten T, Bhati MT, Charbonnier D, Gur RC (2007) Facial emotion recognition in schizophrenia: when and why does it go awry? Schizophr Res 94:253–263.

Vidyasagar TR (1999) A neuronal model of attentional spotlight: parietal guiding the temporal. Brain Res Brain Res Rev 30:66–76.

Wetherill GB, Levitt H (1965) Sequential estimation of points on a psychometric function. Br J Math Stat Psychol 18:1–10.

Whalley HC, Simonotto E, Moorhead W, McIntosh A, Marshall I, Ebmeier KP, Owens DG, Goddard NH, Johnstone EC, Lawrie SM (2006) Functional imaging as a predictor of schizophrenia. Biol Psychiatry 60:454–462.

Yeap S, Kelly SP, Sehatpour P, Magno E, Javitt DC, Garavan H, Thakore JH, Foxe JJ (2006) Early visual sensory deficits as endophenotypes for schizophrenia: high-density electrical mapping in clinically unaffected first-degree relatives. Arch Gen Psychiatry 63:1180–1188.